

# The origin of SFOAE microstructure in the guinea pig

Shawn S. Goodman<sup>a</sup>, Robert H. Withnell<sup>a,\*</sup>, Christopher A. Shera<sup>b</sup>

<sup>a</sup> Department of Speech and Hearing Sciences, Indiana University, 200 South Jordan Avenue, Bloomington, IN 47405, USA

<sup>b</sup> Eaton-Peabody Laboratory, Massachusetts Eye and Ear Infirmary, 243 Charles Street, Boston, MA 02114, USA

Received 12 April 2003; accepted 5 June 2003

## Abstract

Human stimulus-frequency otoacoustic emissions (SFOAEs) evoked by low-level stimuli have previously been shown to have properties consistent with such emissions arising from a linear place-fixed reflection mechanism with SFOAE microstructure thought to be due to a variation in the effective reflectance with position along the cochlea [Zweig and Shera, *J. Acoust. Soc. Am.* 98 (1995) 2018–2047]. Here we report SFOAEs in the guinea pig obtained using a nonlinear extraction paradigm from the ear-canal recording that show amplitude and phase microstructure akin to that seen in human SFOAEs. Inverse Fourier analysis of the SFOAE spectrum indicates that SFOAEs in the guinea pig are a stimulus level-dependent mix of OAEs arising from linear-reflection and nonlinear-distortion mechanisms. Although the SFOAEs are dominated by OAE generated by a linear-reflection mechanism at low and moderate stimulus levels, nonlinear distortion can dominate some part of, or all of, the emission spectrum at high levels. Amplitude and phase microstructure in the guinea pig SFOAE is evidently a construct of (i) the complex addition of nonlinear-distortion and linear-reflection components; (ii) variation in the effective reflectance with position along the cochlea; and perhaps (iii) the complex addition of multiple intra-cochlear reflections.

© 2003 Elsevier B.V. All rights reserved.

**Key words:** Microstructure; Otoacoustic emission; SFOAE

## 1. Introduction

When a low-level tone of constant amplitude is swept across frequency, healthy ears manifest a ‘microstructure’ in ear-canal sound pressure level attributed to the generation of sound by the inner ear (e.g. Zwicker and Schloth, 1984). Such a microstructure can arise in a number of different ways. The total ear-canal pressure at the stimulus frequency ( $P_{ec}$ ) consists of the stimulus pressure ( $P_{stim}$ ) and the pressure from the stimulus-frequency otoacoustic emission (SFOAE) evoked by the stimulus ( $P_{sfe}$ ), i.e.:

$$P_{ec} = P_{stim} + P_{sfe}$$

If  $P_{stim}$  is held constant, then microstructure in  $|P_{ec}|$

will arise if either the amplitude or the phase of  $P_{sfe}$  varies with frequency. In the former case,  $|P_{sfe}|$  itself manifests microstructure. In the latter, the relative phases of  $P_{stim}$  and  $P_{sfe}$  rotate with frequency, creating an interference pattern in  $|P_{ec}|$ . In this case, the microstructure only appears in  $|P_{ec}|$ , not in  $|P_{sfe}|$ .

Measurements of SFOAEs show that, in general, both the amplitude and phase of  $P_{sfe}$  vary with frequency (e.g. Kemp and Chum, 1980; Zwicker and Schloth, 1984; Shera and Zweig, 1993). In this paper we explore the origin of the variation in  $P_{sfe}$  amplitude in the guinea pig ear. In particular, we investigate whether the variation in SFOAE pressure ( $P_{sfe}$ ) can be ascribed solely to a variation in the effective ‘reflection coefficient’ (Zweig and Shera, 1995) or if  $P_{sfe}$  might, in addition, consist of two components whose relative phases vary rapidly with frequency. According to the modeling work of Talmadge et al. (2000), two such components in  $P_{sfe}$  are expected on theoretical grounds, at least at sufficiently high stimulus intensities. According to their model,  $P_{sfe}$  at low levels is dominat-

\* Corresponding author. Tel.: +1 (812) 855 9339;

Fax: +1 (812) 855 5531.

E-mail addresses: [shgoodma@indiana.edu](mailto:shgoodma@indiana.edu) (S.S. Goodman), [rwithnel@indiana.edu](mailto:rwithnel@indiana.edu) (R.H. Withnell), [shera@epl.meei.harvard.edu](mailto:shera@epl.meei.harvard.edu) (C.A. Shera).

ed by a reflection-source OAE that arises by linear coherent reflection from pre-existing mechanical impedance perturbations ('roughness'). The phase of this component rotates rapidly with frequency (Shera and Guinan, 1999). At higher stimulus levels, however, nonlinearities in the mechanics can induce distortion-source OAEs whose phase is almost constant across frequency. If both reflection- and distortion-source OAE components are generated, they will interfere with one another and create an SFOAE microstructure analogous to that seen in distortion-product OAEs (DPOAEs; e.g., Kaluri and Shera, 2001).

## 2. Materials and methods

### 2.1. Animal surgery

Albino guinea pigs (300–650 g) were anesthetized with Nembutal (30–35 mg/kg i.p.) and atropine (0.06–0.09 mg i.p.), followed approximately 15 min later by Hypnorm (0.1–0.15 ml i.m.). Neuroleptanaesthesia was maintained with supplemental doses of Nembutal and Hypnorm. In a number of animals, pancuronium (0.15 ml i.m.) was administered to reduce physiological noise associated with spontaneous muscle contractions. Guinea pigs were tracheotomized and mechanically ventilated on Carbogen (5% CO<sub>2</sub> in O<sub>2</sub>) with body rectal temperature maintained at approximately 37.5°C. The head was positioned using a custom-made head holder that could be rotated for access to the ear canal. Heart rate was monitored throughout each experiment. The bulla was opened dorso-laterally and a silver wire electrode placed on the round window niche for the recording and monitoring of the compound action potential.

### 2.2. Signal generation and data acquisition

SFOAEs were recorded with stimulus delivery and response acquisition computer controlled using custom-software with a Card Deluxe soundcard.

Methods for stimulus delivery and response acquisition have been described previously (Withnell et al., 1998; Withnell and Yates, 1998). Briefly, the acoustic stimulus was delivered by a Beyer DT48 loudspeaker placed approximately 4 cm from the entrance to the ear canal. Ear-canal sound pressure recordings were made by a Sennheizer MKE 2-5 electrostatic microphone fitted with a metal probe tube (1.2 mm long, 1.3 mm i.d., 1500Ω acoustic resistor) positioned in the ear canal approximately 2 mm from the ear-canal entrance. The microphone and probe tube combination was calibrated against a Bruel and Kjaer 1/8 inch microphone. The output from the probe tube microphone was amplified 20 dB, high-pass filtered (0.64 kHz, 4 pole

Butterworth) and transmitted as a balanced input to one of the analogue input channels of the computer sound card (total gain = 30 dB). It was subsequently digitized in ~46 or 93 ms epochs at a rate of 44.1 or 48 kHz (2048 or 4096 points for the fast Fourier transform (FFT)).

The stimulus was a digitally generated tone-burst of 25, 35 or 45 ms duration with 5 ms cosine ramps, the analogue output buffered by a Tucker-Davis Technologies HB6 loudspeaker buffer-amplifier. SFOAEs were extracted using a nonlinear extraction paradigm (Kemp et al., 1990) from the ear-canal sound pressure recordings made in response to a stimulus train with a 6 dB difference between the lower-level (probe level) and higher-level (reference level) stimuli (the stimulus train consisted of two probe level and one reference level tone-bursts). The extraction of the OAE is dependent upon a nonlinear growth of the emission with increasing stimulus level (Kemp et al., 1990). Previous findings in guinea pig using a suppression method (Brass and Kemp, 1991, 1993) support this assumption (Souter, 1995). The extraction of the emission by virtue of its nonlinear growth does not exclude examining a component of linear origin: an OAE of linear origin, e.g. linear place-fixed reflection, can have nonlinear growth by virtue of the compressively nonlinear growth of the basilar membrane (Shera and Guinan, 1999). A limitation of the nonlinear extraction technique is that the extraction of the emission in the ideal case relies on the amplitude of the emission evoked by the higher-level or reference stimulus being similar in amplitude to the emission evoked by the lower-level stimulus, i.e. the emission amplitude is at its maximum value or it has saturated. If the emission amplitude is still growing, then the reference stimulus will evoke an emission larger in amplitude than that evoked by the lower-level stimulus, and the subsequently derived emission will be underestimated.

SFOAEs were obtained within the frequency range 1–19 kHz, with frequency increments of 86 Hz or 172 Hz. SFOAEs were also examined versus stimulus-intensity level over a frequency range of about 3 kHz. The noise floor for SFOAE recordings was calculated as the mean of amplitude densities from ±500 to 1000 Hz from the stimulus frequency.

Measurements in a cavity suggested that intermodulation distortion produced by harmonics of the stimulus tone at the SFOAE frequency was more than 20 dB below the level of the measured OAE for the highest level of stimulus used in this study.

### 2.3. Data analysis

The components of the SFOAE were extracted from the SFOAE complex amplitude spectrum using Fourier

analysis, the SFOAE complex amplitude data windowed using a moving-average Hanning window prior to Fourier analysis. This method of data analysis has been described previously (see Withnell et al., 2003). In brief:

If  $D(f)$  is the complex amplitude data set for all frequencies between  $a$  and  $b$  with a step-size between frequencies of  $\Delta$ , and  $s$  is the sampling rate, then:

$$G(f) = \begin{cases} D(f) & \text{for } a \leq f \leq b \\ 0 & \text{for } -s/2 \leq f < a \quad \text{or } b < f \leq s/2 \end{cases}$$

i.e. the data set has been zero-buffered.  $G(f)$  was then multiplied by a moving Hanning window with an inverse FFT (IFFT) calculated on each windowed data set, i.e.:

$$H_d(t) = \sum G(f) \cdot h_d(f) e^{2\pi i f t}$$

where:

$$h_d(f) = \begin{cases} 0.5 - 0.5 \cos([2\pi(f-p+k\Delta)]/(k\Delta)) & \text{for } [-s/2 + (p-k\Delta)] \leq f \leq [-s/2 + p] \\ 0 & \text{otherwise} \end{cases}$$

and  $p = [(d+1)/2]k\Delta$ ,  $d = 1, 2, 3, \dots, [(2s/(k\Delta)) - 1]$  for a window of size  $k\Delta$ .

Time-domain windowing to separate components with disparate phase behaviors manifesting as temporally discrete responses in the IFFT was performed using a recursive exponential filter developed by Shera and Zweig (see Kalluri and Shera, 2001, Shera and Zweig, 1993), i.e.:

$$\text{SFOAE short-latency component} = H_d(t) \cdot F(t)$$

where  $F(t) = 1/\Gamma_n(\tau/\tau_{\text{cut}})$ , where  $\tau_{\text{cut}}$  is the length of the window and  $\Gamma_n(\tau)$  is defined recursively as:

$$\Gamma_{n+1}(\tau) = e^{\Gamma_n(\tau)-1}, \text{ with } \Gamma_n(\tau) = e^{\tau^2}$$

$\tau_{\text{cut}}$  varied in value over the range of windowed data sets within a given data set subjected to Fourier analysis.  $\tau_{\text{cut}}$  was chosen with the goal of minimizing the phase rotation of the extracted short-latency component. Note that we set Shera and Zweig's scale factor equal to 1:

$$\text{IFFT time-domain waveform} = |H_d(t) \cdot F(t)|$$

$$\text{SFOAE long-latency component} = H_d(t) - H_d(t) \cdot F(t)$$

### 3. Results

Fig. 1 shows three examples of SFOAE amplitude

and phase microstructure recorded from three different animals. The phase in each of the panels shows steps or a change in slope at frequencies corresponding to amplitude minima. This type of phase pattern is consistent with an OAE arising from an interaction between two components, one of which has a phase that varies rapidly with respect to the other (Talmadge et al., 1999). However, a similar phase pattern can also arise without such an interaction between two components, being due to a variation in effective reflectance with position along the cochlea (Zweig and Shera, 1995). Fig. 2 shows similar SFOAE microstructure in data from a human subject (from figure 9 of Shera and Guinan, 1999). Although the data are limited, in neither species do the frequency spacings between adjacent amplitude minima show any regular dependence on emission frequency. Although attributing microstructure entirely to one cause is probably an oversimplification, we note that these data differ from the predictions of the simplest two-component model, in which a regular interference pattern is created through the interaction of two components whose relative phases vary uniformly with frequency.

Fourier analysis of the data in Figs. 1 and 2 allows further exploration of the origin(s) of SFOAE amplitude and phase microstructure.

#### 3.1. IFFT analysis

IFFT analysis and time-domain windowing provides for the separation of components of an OAE that have phase properties that translate into components that are separable in time. Using a sweep-frequency paradigm, a component that arises from a wave-fixed mechanism will have negligible phase rotation and will appear in the IFFT time-domain waveform as the response at and soon after time zero. Violations of scaling symmetry<sup>1</sup> will produce greater phase rotation for a wave-fixed or nonlinear-distortion component, resulting in this component appearing at some time after time zero. Time-domain windowing of the IFFT of Hanning-windowed subsets of the complex amplitude data set – with a cut-off value for the window (the recursive exponential filter) chosen to minimize the phase rotation of the short-latency component – separates the short-latency component from the long-latency component/s. The place-fixed component of an OAE is thought to arise from reflection from impedance inhomogeneities fixed in position on the basilar membrane; it has a phase that rotates rapidly with frequency, the phase-gradient being an estimate of the group delay for this component (Kal-

<sup>1</sup> For example, due to place-fixed impedance inhomogeneities along the basilar membrane.

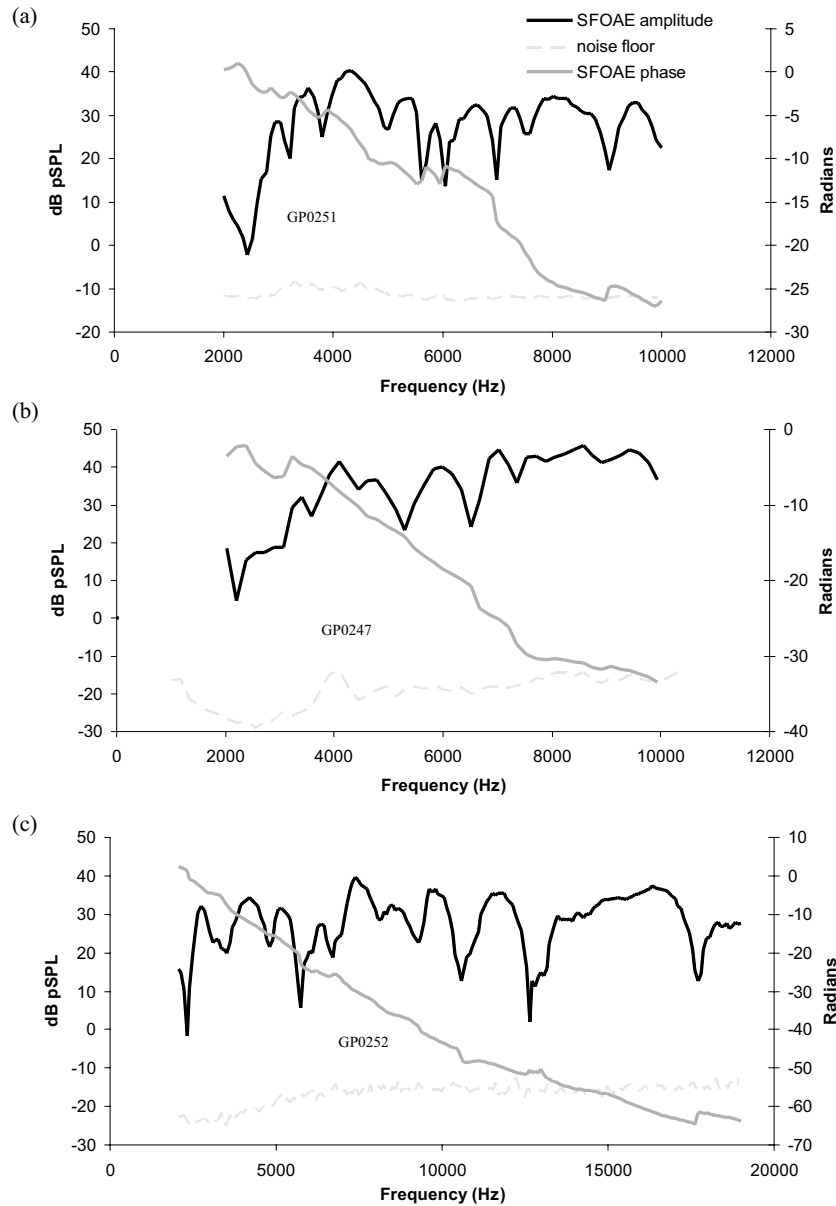


Fig. 1. Three examples of SFOAE amplitude and phase microstructure recorded from three different animals. Note that the phase in each of the figures shows a step or change in slope corresponding to amplitude minima, such features being consistent with two components, one of which has a phase that varies rapidly with respect to the other. Stimulus probe levels were 74, 80 and 73 dB pSPL, respectively.

luri and Shera, 2001). This place-fixed component will appear as long-latency components or later peaks in the IFFT time-domain waveform. Previous SFOAE measurements in guinea pig at stimulus levels of 40 dB SPL and below suggest that this OAE arises as a result of a linear coherent reflection mechanism (Shera and Guinan, 2003).

Separation of components based on their temporal properties into a short- and a long-latency component using Fourier analysis and time-domain windowing of the SFOAE from one of the animals in Fig. 1 is shown in Fig. 3. The characteristic of an OAE comprised of two components arising from different mechanisms is

that one of the components has a phase that is approximately constant versus frequency (4 radians over 2.3 octaves) and is consistent with a component arising from a nonlinear-distortion mechanism, while the other component has a phase that varies 44 radians over 2.3 octaves, consistent with a component arising from a place-fixed mechanism. The slowly varying phase or short-latency component has a magnitude that, for this animal, is typically less than the magnitude of the long-latency component, being greater in amplitude than the long-latency component only from 7700 to 9600 Hz. Consistent with the slowly varying phase component dominating the OAE over this frequency range,

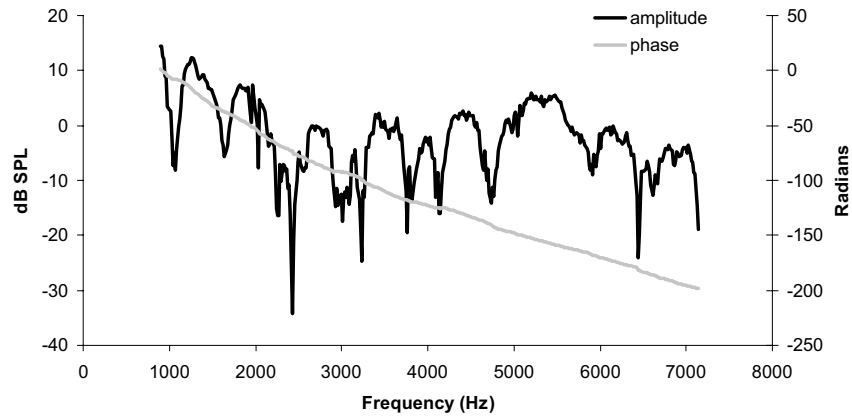


Fig. 2. SFOAE amplitude and phase recorded from a human subject in response to a 40 dB SPL stimulus (55 dB SPL suppressor) using a variant of the suppression paradigm of Brass and Kemp. Data courtesy of [Shera and Guinan \(1999, figure 9\)](#). The phase appears to be a smoothly rotating function of frequency, i.e. microstructure is present but it is small relative to the rate of rotation of the phase.

the slope of the phase of the SFOAE is less from 7700 to 9600 Hz than below 7700 Hz. [Fig. 4](#) shows the individual IFFT time-domain waveforms (i.e. the magnitude of the IFFTs) corresponding to the data of [Fig. 3](#). IFFTs were obtained with Hanning windows approximately 2060 Hz wide. A frequency spacing of 172 Hz between data points for this particular data set limits the time-domain measurement to 2.9 ms. There is no

evidence in any of the panels of more than one reflection, i.e. no later intra-cochlear reflections. The absence of any significant later reflection components in the IFFT time-domain waveforms argues for the microstructure for the long-latency component in [Fig. 3](#) to arise from a variation in the effective reflectance with position along the cochlea.

[Fig. 5](#) shows the corresponding IFFT time-domain

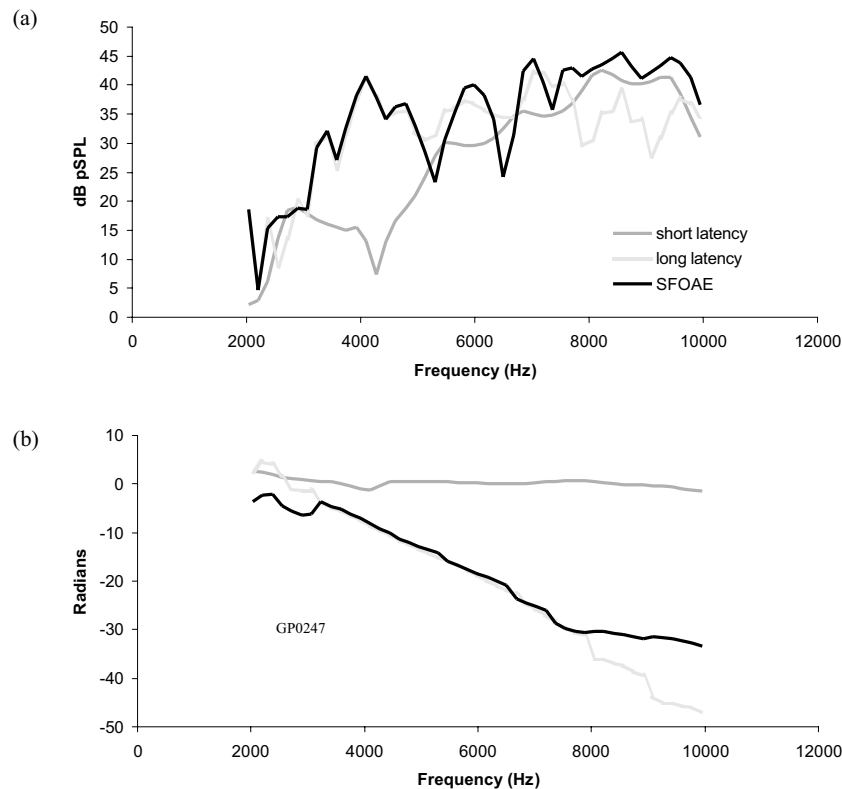


Fig. 3. Amplitude and phase of an SFOAE and the two components that comprise the SFOAE extracted using IFFT analysis and time-domain windowing. Stimulus probe level was 80 dB pSPL. The characteristic of an OAE comprised of two components arising from different mechanisms is that the phase of one component is approximately constant versus frequency while the other component has a phase that varies rapidly versus frequency.

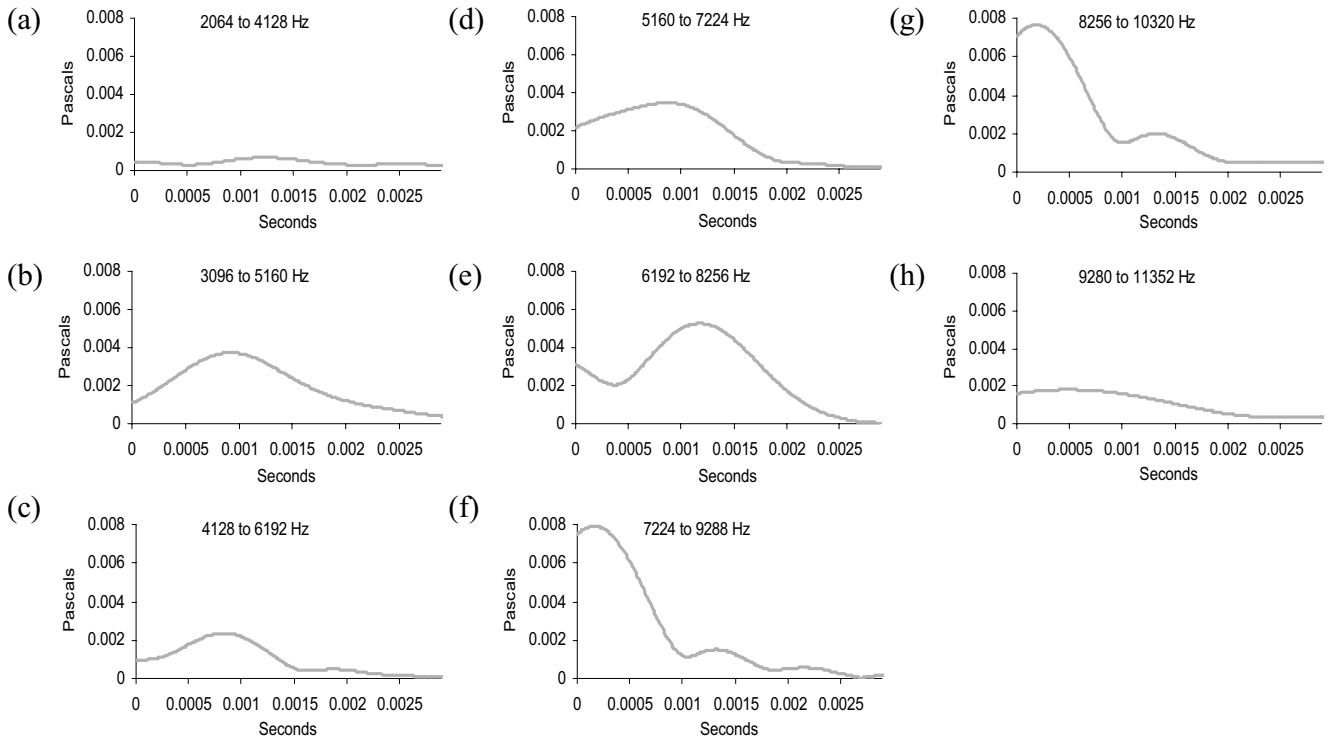


Fig. 4. Individual IFFT time-domain waveforms corresponding to the data of Fig. 3. There is no evidence in any of the panels of more than one reflection, i.e. no later intra-cochlear reflections.

waveforms for the human data of Fig. 2. IFFTs were obtained with Hanning windows 390 Hz wide. Thirty-three IFFT time-domain waveforms were obtained from data over the frequency range 893–7148 Hz,

shown in four panels in Fig. 5. Most of these time-domain waveforms have only a single peak corresponding to one reflection component. In four cases there is evidence of a second reflection component (thickened

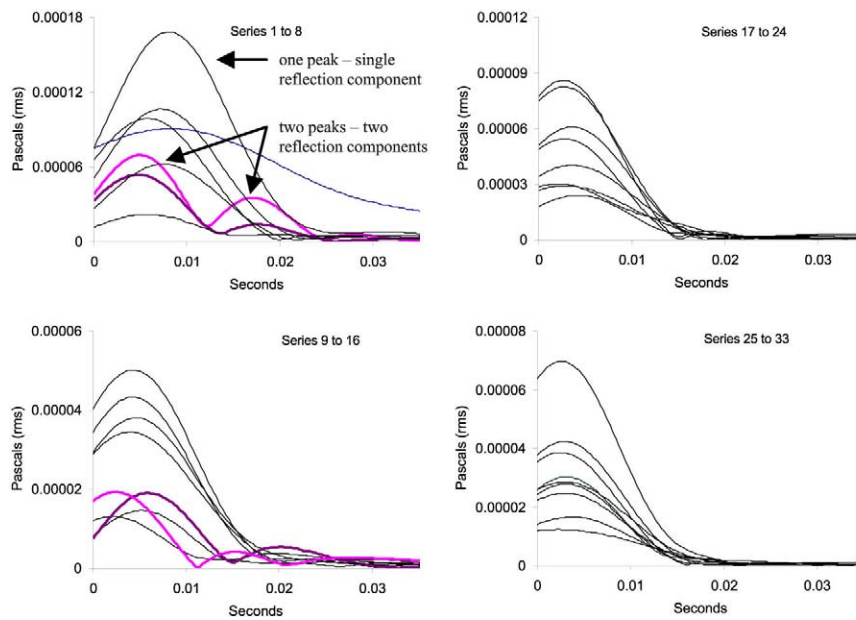


Fig. 5. IFFT time-domain waveforms corresponding to the human data of Fig. 2. Thirty-three IFFT time-domain waveforms were obtained from data over the frequency range 893–7148 Hz. Most of these time-domain waveforms have only a single peak corresponding to one reflection component. In four cases, the IFFT time-domain waveform has two peaks, these corresponding to IFFTs calculated over the frequency regions 893–1283 Hz, 1478–1868 Hz, 3038–3428 Hz, and 4793–5183 Hz.

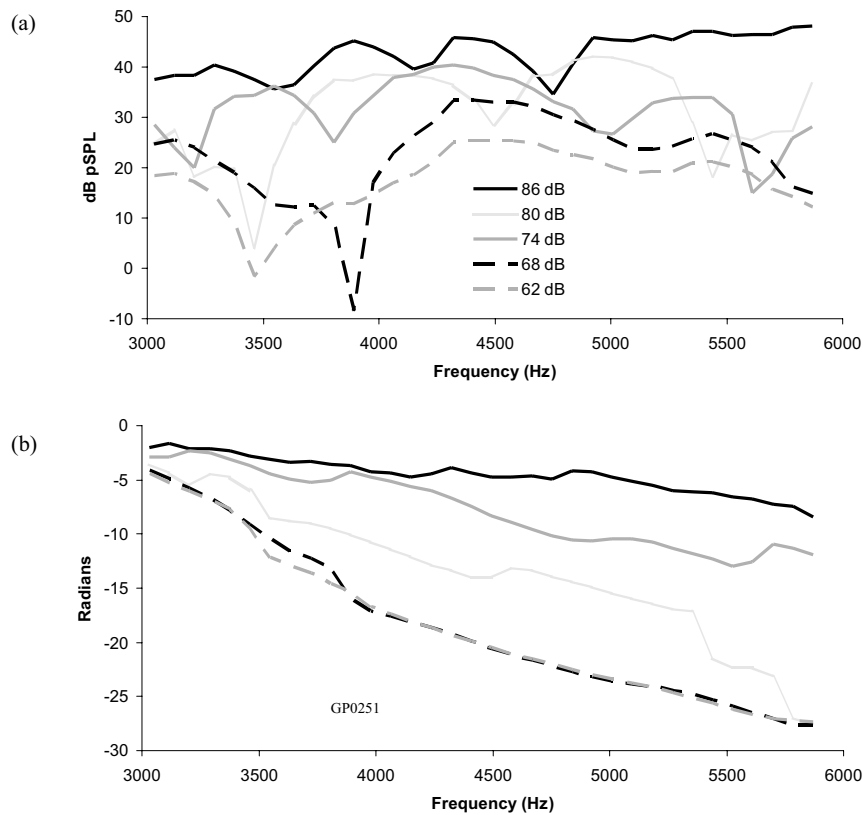


Fig. 6. SFOAE amplitude (panel a) and phase (panel b) versus frequency obtained over a range of stimulus levels from a guinea pig. Amplitude microstructure is present but such a microstructure varies with stimulus level. The phase response to the highest level stimulus has a shallower slope than that obtained at lower stimulus levels (see text for further discussion). The  $S/N$  ranged from 11 to 60 dB.

curves), but the fact that in most waveforms there are no later reflections strongly suggests that, as for the long-latency component of Fig. 3a, the SFOAE amplitude microstructure of Fig. 2 is predominantly due to a variation in the effective reflectance with position along the cochlea.

### 3.2. Stimulus-intensity effects

Fig. 6 shows an example of SFOAE amplitude and phase versus frequency obtained over a range of stimulus levels from a guinea pig. SFOAE amplitude microstructure is evident at all stimulus levels but such a microstructure varies in a manner that is stimulus level-dependent. At probe levels of 62 and 68 dB pSPL, the amplitude microstructure appears less than that obtained at higher levels; the response for 62 dB pSPL, for instance, has only one pronounced amplitude minimum at 3460 Hz while the response to the 80 dB pSPL stimulus has three pronounced amplitude minima. At 86 dB pSPL, amplitude microstructure appears reduced relative to the 74 and 80 dB pSPL responses. The phase responses show microstructure consistent with amplitude measurements, phase transitions (steps or changes in the slope of the phase) occurring in the frequency

regions of the amplitude minima. At 86 dB pSPL the emission phase rotates 6 radians over 3 kHz while at 62 dB pSPL it rotates 23 radians over the same frequency range. This variation in the amount of phase accumulation is consistent with two components with disparate phase properties contributing to the OAE and a shift in the relative contributions of the two components.

Using IFFT analysis and time-domain windowing, the SFOAEs of Fig. 6 are separated into short- and long-latency components in Fig. 7. At the highest stimulus level, the SFOAE is dominated by the short-latency component or component with slowly rotating phase; at lower stimulus levels the SFOAE appears to be dominated by a component with rapidly rotating phase, i.e. arising from a place-fixed reflection mechanism. The amplitude microstructure of the SFOAE evoked by stimulus levels of 62–80 dB pSPL is similar to, but not exactly the same as, the long-latency component. That is, the short-latency component arising from a nonlinear-distortion mechanism appears to contribute to SFOAE amplitude microstructure at these stimulus levels. The OAE component attributed to arise from a linear place-fixed reflection mechanism at the highest stimulus level has a different pattern to that observed at lower stimulus levels; perhaps this suggests

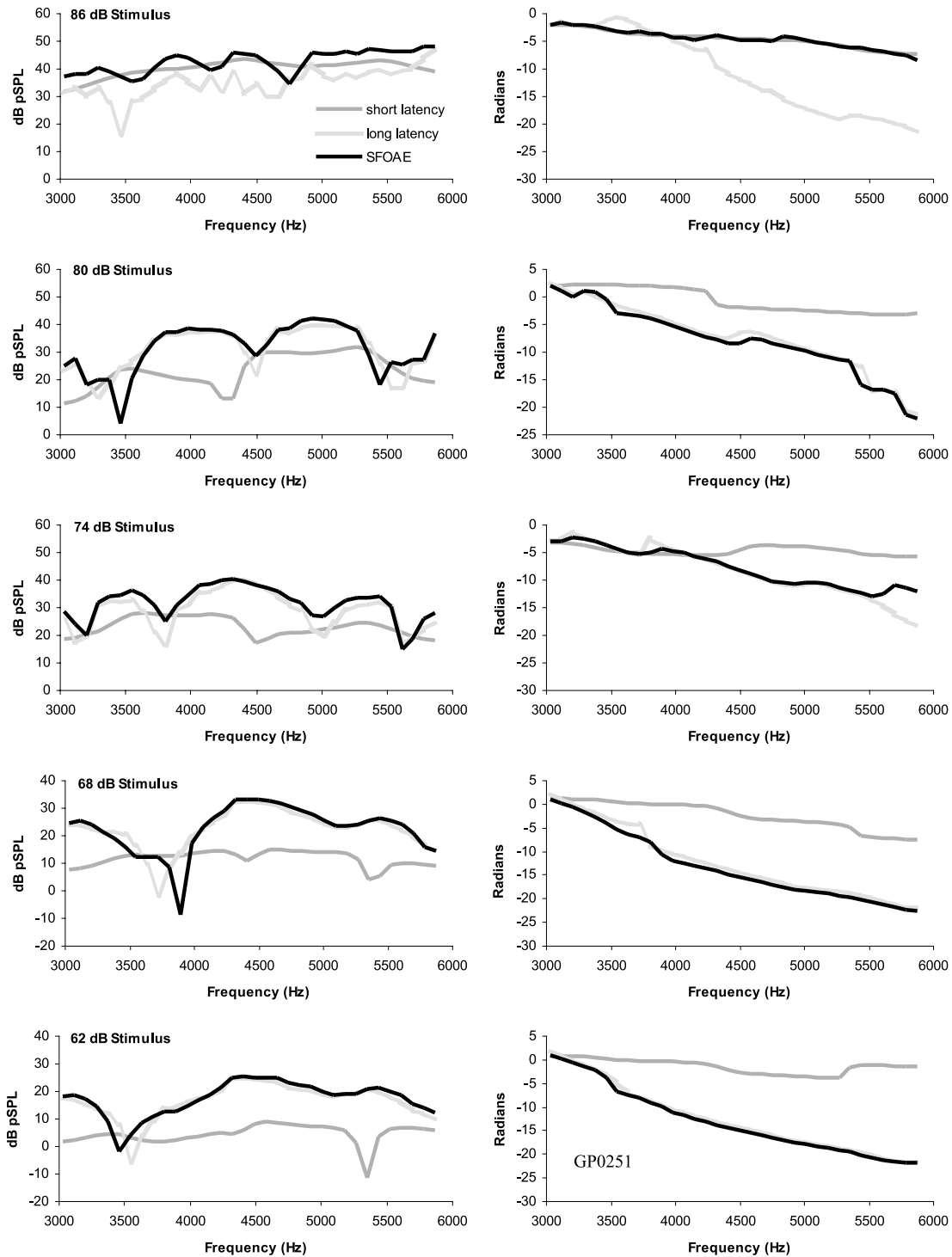


Fig. 7. Amplitude and phase of SFOAEs at each of five stimulus levels (data of Fig. 3) and the two components of each SFOAE extracted using IFFT analysis and time-domain windowing. At the highest stimulus level, the SFOAE is dominated by a component with slowly rotating phase, presumably nonlinear distortion; at lower stimulus levels it appears to be dominated by a component arising from a reflection mechanism. In each case, there are two components present, one having a slowly rotating phase, the other a rapidly rotating phase.

a stimulus level-dependent limitation to the application of the theory of linear coherent reflection.

Examination of the slope of the phase of the long-latency component versus stimulus level suggests no

systematic level-dependent change in group delay as might be expected given a broadening of the traveling wave envelope with increasing stimulus level (Zweig and Shera, 1995). One possible explanation for this perhaps

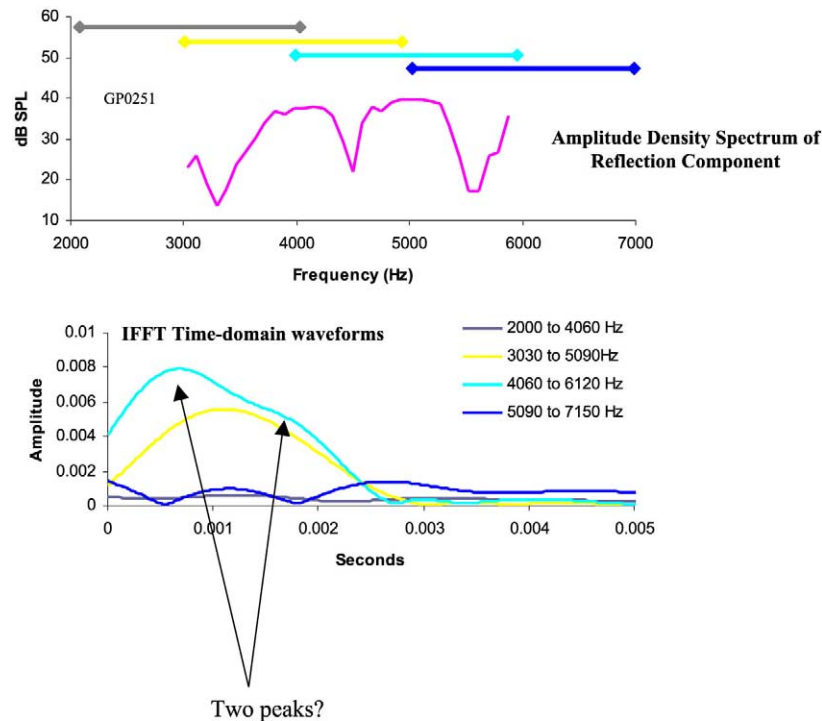


Fig. 8. Amplitude density spectrum for the reflection component of the SFOAE in response to a 74 dB pSPL stimulus from GP0251 and the corresponding IFFT time-domain waveforms. Later intra-cochlear reflections may be suggested in one of the IFFT time-domain waveforms but such interpretation is equivocal.

counter-intuitive finding is that at higher stimulus levels the coherence provided by spatial tuning may be affected. With increasing stimulus level, the peak of the traveling wave broadens resulting in:

1. a larger distribution of irregularities being encompassed within this peak region, complicating the sum of the scattered wavelets reflected from the individual irregularities;
2. the wavelength of the traveling wave may vary more over the region of scattering than it does at lower stimulus levels, where the peak of the traveling wave is more spatially confined.

### 3.3. Multiple intra-cochlear reflections

Standing waves in the cochlea produced by reflection between the stapes footplate and the region of origin in the cochlea of the OAE generate an OAE measured in the ear canal that is a composite of these standing waves or intra-cochlear reflections, resulting in an amplitude and phase microstructure (Dhar et al., 2002). We examine this for one animal in Fig. 8. Fig. 8 (top panel) shows the amplitude density spectrum of the total reflection component and has horizontal bars to show the regions over which IFFTs were calculated. There is a suggestion in the IFFT time-domain waveforms of panel b of two reflection peaks in one of the IFFT time-domain waveforms. Such later peaks, if they

do indeed represent later intra-cochlear reflections, would alter OAE microstructure (Dhar et al., 2002). While such later peaks are often seen in IFFT time-domain waveforms from human OAEs (e.g. Shera and Zweig, 1993), our data are equivocal and it may be that multiple intra-cochlear reflections are not commonly present in guinea pig OAEs.

## 4. Discussion

OAEs are believed to arise from two distinct generating mechanisms, a linear place-fixed reflection mechanism and a nonlinear wave-related distortion mechanism, both mechanisms being dependent on the action of the cochlear amplifier for the production of detectable OAEs (Shera and Guinan, 1999). A linear place-fixed reflection mechanism is thought to involve the forward traveling wave being reflected from spatially random inhomogeneities or impedance discontinuities distributed along the cochlear partition (Zweig and Shera, 1995; Talmadge et al., 1998; Shera, 2003). Such a mechanism is presumed to be dominant at low stimulus levels (see Zweig and Shera, 1995). The OAE arising out of a nonlinear wave-related distortion mechanism is presumably predominantly energy propagating out to the ear canal as a result of forces associated with outer hair cell electromechanical transduction coupling

into the cochlear fluids via the basilar membrane, although a nonlinear-reflection mechanism has also been posited (Talmadge et al., 2000).

DPOAEs in humans have been shown to arise from the complex interaction of components coming from two different locations on the basilar membrane (Heitmann et al., 1998), with different generating mechanisms dominating the production of each component (Talmadge et al., 1999; Kalluri and Shera, 2001). A consequence of DPOAEs arising from multiple components with different phase behaviors is that DPOAEs show amplitude and phase microstructure versus frequency. SFOAEs from humans have also been shown to demonstrate amplitude and phase microstructure (Shera and Guinan, 1999); however, in this case the microstructure was attributed to a variation in the effective reflectance with position along the cochlea and not an interaction between multiple components with different phase slopes.

In the guinea pig, SFOAE microstructure appears to be a composite of two and perhaps three different contributions:

1. the complex addition of two components with differing phase properties, i.e. as is seen with DPOAEs, recording the OAE versus frequency for a constant stimulus level produces a component with a slowly rotating phase<sup>2</sup> and a component with a rapidly rotating phase, i.e. two components arising from different generating mechanisms,
2. a variation in the effective reflectance with position along the cochlea, and perhaps
3. the complex addition of multiple intra-cochlear reflections

At most stimulus levels, the component arising from a linear-reflection mechanism dominates the ear-canal recorded OAE, the contribution from each of the mechanisms being level-dependent. However, at sufficiently high stimulus levels (e.g. 86 dB pSPL in Fig. 7) the short-latency component presumably arising from a nonlinear-distortion mechanism can dominate the recorded OAE.

Although our sample size is relatively small, multiple intra-cochlear reflections seem to be less evident in guinea pig OAEs than human OAEs. Such later reflections could contribute to amplitude and phase microstructure, although unequivocal evidence for such a contribution is lacking. Indeed, the absence of multiple intra-cochlear reflections and the fact that the guinea pig cochlea seldom has SOAEs may suggest that the impedance mismatch between the cochlea and middle ear is smaller in guinea pig than it is in humans and/or

that there is less irregularity in the guinea pig cochlea contributing to reflection-source OAEs.

A caveat to the interpretation of the origin of the SFOAE in guinea pig is that a harmonic mechanism (Fahey et al., 2000), whereby intermodulation distortion at the SFOAE frequency is produced by the nonlinear interaction on the basilar membrane of the second and third harmonics of the stimulus tone (producing a quadratic difference tone) and/or harmonics generated within the cochlea, may contribute to the ear-canal recorded SFOAE, especially at higher stimulus levels. This component, if present, may have both wave and place-fixed components. Stimulus-related harmonic distortion was at least 45 dB below the stimulus tone and so any intermodulation distortion OAE that could arise is unlikely to contribute significantly to the SFOAE. Harmonics generated within the cochlea could conceivably produce a quadratic difference tone at the SFOAE frequency; further research is necessary to evaluate what contribution, if any, such a mechanism might make.

One might infer from the findings of this paper that SFOAE microstructure is more complex than DPOAE microstructure. However, Kalluri and Shera (2001) have shown the equivalence between the DPOAE component arising from the DP place and the corresponding SFOAE (at least in humans at low to moderate sound levels and an  $f_2/f_1$  of approximately 1.2). Based on this, we infer that the DPOAE component from the DP place will, in principle, have the same properties as that observed here for the SFOAE, such complexity not being apparent due to the level-dependent nature of the contributions of the various components.

## Acknowledgements

This work was supported by NIH-NIDCD DC04921 (R.H.W.), by NIH-NIDCD T32 DC00012 Training Grant (S.S.G.), and by NIH-NIDCD DC03687 (C.A.S.). Portions of this paper were presented at the Association for Research in Otolaryngology Mid-Winter Meeting, 2003.

## References

- Brass, D., Kemp, D.T., 1991. Time-domain observation of otoacoustic emissions during constant tone stimulation. *J. Acoust. Soc. Am.* 90, 2415–2427.
- Brass, D., Kemp, D.T., 1993. Suppression of stimulus frequency otoacoustic emissions. *J. Acoust. Soc. Am.* 93, 920–939.
- Dhar, S., Talmadge, C.L., Long, G., Tubis, A., 2002. Multiple internal reflections in the cochlea and their effect on DPOAE fine structure. *J. Acoust. Soc. Am.* 112, 2882–2897.
- Fahey, P.F., Stagner, B.B., Lonsbury-Martin, B.L., Martin, G.K.,

<sup>2</sup> By virtue of wave-scaling (Talmadge et al., 1998; Shera and Guinan, 1999).

2000. Nonlinear interactions that could explain distortion product interference response areas. *J. Acoust. Soc. Am.* 108, 1786–1802.
- Heitmann, J., Waldmann, B., Schnitzler, H., Plinkert, P.K., Zenner, H., 1998. Suppression of distortion product otoacoustic emissions (DPOAE) near  $2f_1 - f_2$  removes DP-gram microstructure – evidence for a secondary generator. *J. Acoust. Soc. Am.* 103, 1527–1531.
- Kalluri, R., Shera, C.A., 2001. Distortion-product source unmixing: A test of the two-mechanism model for DPOAE generation. *J. Acoust. Soc. Am.* 109, 622–637.
- Kemp, D.T., Chum, R., 1980. Properties of the generator of the stimulated acoustic emissions. *Hear. Res.* 2, 533–548.
- Kemp, D.T., Ryan, S., Bray, P., 1990. A guide to the effective use of otoacoustic emissions. *Ear Hear.* 11, 93–105.
- Shera, C.A., 2003. Wave interference in the generation of reflection- and distortion-source emissions. In: Gummer, A.W. (Ed.), *Biophysics of the Cochlea: From Molecule to Model*. World Scientific, Singapore, pp. 439–449.
- Shera, C.A., Guinan, J.J., 2003. Stimulus-frequency-emission group delay: A test of coherent reflection filtering and a window on cochlear tuning. *J. Acoust. Soc. Am.* 113, 2762–2772.
- Shera, C.A., Guinan, J.J., 1999. Evoked otoacoustic emissions arise by two fundamentally different mechanisms: A taxonomy for mammalian OAEs. *J. Acoust. Soc. Am.* 105, 782–798.
- Shera, C.A., Zweig, G., 1993. Noninvasive measurement of the cochlear traveling-wave ratio. *J. Acoust. Soc. Am.* 93, 3333–3352.
- Souter, M., 1995. Stimulus frequency otoacoustic emissions from guinea pig and human subjects. *Hear. Res.* 90, 1–11.
- Talmadge, C.L., Tubis, A., Long, G.R., Piskorski, P., 1998. Modeling otoacoustic emission and hearing threshold microstructures. *J. Acoust. Soc. Am.* 104, 1517–1543.
- Talmadge, C.L., Long, G.R., Tubis, A., Dhar, S., 1999. Experimental confirmation of the two-source interference model for the microstructure of distortion product otoacoustic emissions. *J. Acoust. Soc. Am.* 105, 275–292.
- Talmadge, C.L., Tubis, A., Long, G.R., Tong, C., 2000. Modeling the combined effects of basilar membrane nonlinearity and roughness on stimulus frequency otoacoustic emission microstructure. *J. Acoust. Soc. Am.* 108, 2911–2932.
- Withnell, R.H., Shaffer, L.A., Talmadge, C.L., 2003. Generation of DPOAEs in the guinea pig. *Hear. Res.* 178, 106–117.
- Withnell, R.H., Kirk, D.L., Yates, G.K., 1998. Otoacoustic emissions measured with a physically open recording system. *J. Acoust. Soc. Am.* 104, 350–355.
- Withnell, R.H., Yates, G.K., 1998. Enhancement of the transient-evoked otoacoustic emission with the addition of a pure tone in the guinea pig. *J. Acoust. Soc. Am.* 104, 344–349.
- Zweig, G., Shera, C.A., 1995. The origin of periodicity in the spectrum of evoked otoacoustic emissions. *J. Acoust. Soc. Am.* 98, 2018–2047.
- Zwicker, E., Schloth, E., 1984. Interrelation of different oto-acoustic emissions. *J. Acoust. Soc. Am.* 75, 1148–1154.